J|A|C|S
ARTICLES
Published on Web 11/01/2002

Free Radical Chemistry of Flavan-3-ols: Determination of Thermodynamic Parameters and of Kinetic Reactivity from Short (ns) to Long (ms) Time Scale

Cécile Cren-Olivé,[†] Philippe Hapiot,[‡] Jean Pinson,[§] and Christian Rolando*[,†]

Contribution from the Laboratoire de Chimie Organique et Macromoléculaire, Equipe Polyphénols, Université des Sciences et Technologies de Lille, UMR CNRS 8009, Bâtiment C4, 59655 Villeneuve d'Ascq Cedex, France, Laboratoire d'Electrochimie Moléculaire et Macromoléculaire, Synthèse et Electrosynthèse Organiques, Université de Rennes 1, UMR CNRS 6510, Campus de Beaulieu, Bat. 10 C, 35042 Rennes Cedex, France, and Laboratoire d'Electrochimie Moléculaire, Université Denis Diderot (Paris 7), UMR CNRS 7591, 2 Place Jussieu, 75251 Paris Cedex 05, France

Received March 20, 2002

Abstract: The physical chemistry and the free radical chemistry of the most abundant polyphenolic flavan-3-ols in food, catechin, its methylated metabolites, and several methylated analogues, have been investigated by laser flash photolysis and cyclic voltammetry studies. Two independent phenoxyl radicals formed upon oxidation of flavan-3-ols have been characterized and identified unambiguously: a short-lived resorcinol-like radical characterized by an absorption band at $\lambda = 495$ nm and a long-lived catechol-like transient absorbing at $\lambda = 380$ nm. The determination of all the thermodynamic constants of each phenolic function of flavan-3-ols, namely, redox potential ($E^{\circ}_{3'} = 0.13_5$ V/SCE, $E^{\circ}_{4'} = 0.11_0$ V/SCE, $E^{\circ}_{5} = 0.28_5$ V/SCE) and microscopic dissociation constants ($pK_{a3'} = 9.02$, $pK_{a4'} = 9.12$, $pK_{a5} = 9.43$, $pK_{a7} = 9.58$) were performed. These values are discussed and compared to the prediction of the density functional theory calculations made on the different species catechin, catechin phenoxyl, and catechin phenolate for each phenolic site.

Introduction

Flavan-3-ols constitute a large class of polyphenolic compounds ubiquitous in plants[1] and so widely found in a number of foods:[2] fruits (apple, apricot, peach ...),[3a] vegetables,[3a] beverages (wine, tea),[3b] and chocolate.[3c] Many epidemiological studies show that consumption of fruits and vegetables is associated with a lowered risk of degenerative diseases such as cancers,[4] cardiovascular diseases,[5] and immune dysfunctions.[6] For example, in western countries, one in ten women will develop breast cancer while in Japan—a country in which drinking green tea that contains a large amount of flavan-3-ols is an integral art of lifestyle—only one in forty women will develop breast cancer.[4f] These epidemiological results are corroborated by many in vitro and in vivo studies demonstrating the impact of flavan-3-ols on mammalian biology[7] and displaying the remarkable scope of biochemical and pharmacological actions of these compounds, among others their antiviral,[8] antiinflamatory,[9] and antiallergic[10] properties. Above all, many

* Corresponding author. Phone: 333 20 43 49 77. Fax: 333 20 33 61 36. E-mail: Christian.Rolando@univ-lille1.fr.
[†] Université des Sciences et Technologies de Lille.
[‡] Université Rennes 1.
[§] Université Denis Diderot (Paris 7).

(1) (a) *The Flavonoïds: Advances in Research Since 1986*; Harbone, J. B., Ed.; Chapman and Hall: London, 1994. (b) Bravo, L. *J. Nutr. Rev.* **1998**, *56*, 317. (c) Kühnau, J. *World Rev. Nutr. Diet* **1976**, *24*, 117. (c) Ferreira, D.; Bekker, R. *Nat. Prod. Rep.* **1996**, *13*, 411. (d) Quideau, S.; Feldman, K. S. *Chem. Rev.* **1996**, *96*, 475. (e) Shahidi, F.; Naczk, M. *Food Phenolics, Sources, Chemistry, Effects, Applications;* Technomic Publishing Co. Inc.: Lancaster, PA, 1995; Vol. 111, pp 125, 331.
(2) (a) Hackett, A. M. *Plant Flavonoïds in Biology and Medecine: Biochemical, Pharmacological, and Structural-Activity Relationships;* Alan R. Liss; New York, 1986; pp 177−194. (b) Macheix, J.-J.; Fleuriet, A. *Fruit Phenolics;* CRC Press: Boca Raton, FL, 1990. (c) Cook, N. C.; Samman, S. *Nutr. Biochem.* **1996**, *7*, 66. (d) Scalbert, A.; Williamson, G. *J. Nutr.* **2000**, *130*, 2073S.
(3) (a) Arts, I. C.; van de Putte, B.; Hollman, P. C. H. *J. Agric. Food Chem.* **2000**, *48*, 1746. (b) Arts, I. C.; van de Putte, B.; Hollman, P. C. H. *J. Agric. Food Chem.* **2000**, *48*, 1752. (c) Arts, I. C.; Hollman, P. C. H.; Kromhout, D. *Lancet* **1999**, *354*, 9177.
(4) (a) Doll, R.; Peto, R. *J. Natl. Cancer Inst.* **1981**, *66*, 1191. (b) Henderson, B. E.; Ross, R. K.; Pike, M. C. *Science* **1991**, *254*, 1131. (c) Ames, B. N.; Gold, L. S.; Willett, W. C. *Proc. Natl. Acad. Sci. U.S.A.* **1995**, *92*, 5258. (d) Hertog, M. G. L.; Hollman, P. C. H.; Katan, M. B.; Kromhout, D. *Nutr. Cancer* **1993**, *20*, 21. (e) Stavric, B. *Clin. Biochem.* **1994**, *27*, 319. (f) Nakachi, K.; Suemasu, K.; Suga, K.; Takeo, T.; Imai, K.; Higashi, Y. *Jpn. J. Cancer Res.* **1998**, *89*, 254.
(5) (a) Renaud, S.; de Lorgeril, M. *Lancet* **1992**, *339*, 1523. (b) de Lorgeril, M.; Salen, P. *Lancet* **1999**, *353*, 1067. (c) Hertog, M. G. L.; Fesken, E. J. M.; Hollman, P. C. H.; Katan, M. B.; Kromhout, D. *Lancet* **1993**, *342*, 1007.
(6) Smith, M. A.; Perry, G.; Richey, P. L.; Sayre, L. M.; Anderson, V. E.; Beal, M. F.; Kowall, N. *Nature* **1996**, *382*, 120−121.
(7) (a) Middleton, E., Jr.; Kandaswami C. In *The Flavonoïds: Advances in Research Since 1986*; Harbone, J. B., Ed.; Chapman and Hall: London, 1994; pp 619−652. (b) Mitscher, L. A.; Jung, M.; Shankel, D.; Dou, J. H.; Steele, L.; Pillai, S. *Med. Res. Rev.* **1997**, *17*, 327. (c) Das, D. K.; Sato, M.; Ray, P. S.; Maulik, G.; Engelman, R. M.; Bertelli, A. A. E.; Bertelli A. *Drugs Exptl. Clin. Res.* **1999**, *25*, 115. (d) Peterson, J.; Dwyer, J. *Nutr. Res.* **1998**, *18*, 1995.
(8) (a) Hanasaki, Y.; Ogawa, S.; Fukui, S. *Free Radical Biol. Med.* **1994**, *16*, 845. (b) Shahat, A. A.; Ismail, S. I.; Hammouda, F. M.; Azzam, S. A.; Lemière, G.; de Bruyne, T.; de Swaef, S.; Pieters, L.; Vlietinck, A. *Phytomedicine* **1998**, *5*, 133. (c) Kakiuchi, N.; Kusumoto, I. T.; Hattori, M.; Namba, T.; Hatano, T.; Okuda, T. *Phytother. Res.* **1991**, *5*, 270.
(9) (a) Saito, M.; Hosoyama, H.; Ariga, T. *J. Agric. Food Chem.* **1998**, *46*, 1460. (b) Hartisch, C.; Kolodzeij, H.; von Bruchausen, F. *Planta Med.* **1997**, *63*, 106.
(10) Hope, W. C.; Welton, A. F.; Fielder-Nagy, C.; Batula-Bernado, C.; Coffey, J. W. *Biochem. Pharmacol.* **1983**, *32*, 367.

of these studies focus on the protective effects of flavan-3-ols against lipid peroxidation and low-density lipoproteins (LDL) oxidation[11] as well as on their antiproliferative and anticarcinogenic actions.[12] Indeed, at low concentration (the sum of the maximum concentrations of catechin, 3′-*O*-methylcatechin, and all conjugates in human plasma is in the range of 91 nmol/L),[13f] catechin, epicatechin, and epigallocatechin gallate have been shown to suppress the formation of lipid peroxidation in biological tissues and subcellular fractions such as microsome and LDL.[11] Others emphasized the growth inhibitory effects of epigallocatechin on various type of cancerous cells (human or animal prostate, mammary, leukemic cells):[12] epigallocatechin inhibits, for example, the growth of human MCF-7 and MDA breast cancer cells but not the growth of their normal counterparts.[12h] So these and related findings explain why flavan-3-ols are considered to be key compounds in the relationship between health and diet.

These protective effects have been mainly attributed to the antioxidative activities of flavan-3-ols[14] and their ability to inhibit enzymes involved in the production of reactive oxygen species.[15] Despite the fact that the ability of flavonoids to act as antioxidant has received a great deal of attention, the mechanism of the observed properties remains far from well-understood. Numerous studies have investigated the chemistry of flavonoid radicals (reduction potentials, pK_a values, spectral properties),[16] the reactivity of these radicals, and the formation of secondary oxidized products.[17] But there is much discussion and contradiction regarding the structure of the phenoxyl radicals,[16b,c,h−j] the reduction potentials,[16b,c,h,g,18] and the structure−activity relationship on the antioxidant activity.[17g,h,j,k] Most of the problems encountered when describing catechin antioxidative activity are due to the lack of information on the intrinsic reactivity of each ring (A, B) and the lack of reliable thermodynamic constants.

Indeed, the thermodynamic constants ($E°$ [16a−e,18] and pK_a[19]) for most dietary polyphenols are still not firmly established or are the subject of controversy. Three ways are open for determining the required constants: experimental measurements, estimation by free energy relationship like Hammett relation, and ab initio or semiempirical calculation. However, all three methods have drawbacks. Classical measurement of pK_a[19a,b] using either UV spectrometry or potentiometry is not able to determine the site of deprotonation on compounds exhibiting several hydroxyl groups such as most of the polyphenols. These methods afford the successive pK_a in the case of polyphenols, whereas the interesting data are the first ionization on each site. Standard potential can be measured by electrochemistry[19] or pulse radiolysis.[16a−e] However, for the two methods, the measurement must be faster than the following reactions induced by the oxidation of the phenol group in order to get reliable thermodynamic value. This is scarcely true, and even the $E°$ value of a simple catechol such as caffeic acid[20] (3-(3,4-dihydroxyphenyl)-2-propenoic acid) cannot be determined using ultrafast cyclic voltammetry on ultramicroelectrodes, whereas coniferyl alcohol (4-(3-hydroxy-1-propenyl)-2-methoxyphenol) is at the limit of the method.[21] In such a situation, the Hammett relationship is most of the time a good method for estimating acidity constants and standard potentials. However, most Hammett correlations involving polyphenols are badly behaved for three reasons: (i) most of the phenol groups bear an ortho substituent, situation in which the Hammett relationship is not relevant,[22] (ii) in water the interesting substituents for polyphenols (mainly hydroxyl and methoxy groups) behave abnormally and cannot be correlated to gas phase or dimethyl sulfoxide (DMSO) solutions, and (iii) most of the time, hydroxyl and

(11) (a) Rankin, S. M.; Hoult, J. R. S.; Leake, D. S. *J. Pharmacol.* **1988**, *95*, 727P. (b) Frankel, E. N.; Kanner, J.; German, J. B.; Parks, E.; Kinsella, J. E. *Lancet* **1993**, *341*, 454. (c) Yang, T. T. C., Koo, M. W. L. *Atherosclerosis* **2000**, *148*, 67. (d) Sanchez-Moreno, C.; Jiménez-Escrig A.; Saura-Calixto F. *Nutr. Res.* **2000**, *20*, 941. (e)Yamanaka, N.; Oda, Osamu; Nagao, S. *FEBS Lett.* **1997**, *401*, 230. (f) Ishikawa, T.; Suzukawa, M.; Ito, T.; Yoshida, H.; Ayaori, M.; Nishiwaki, M.; Yonemura, A.; Hara, Y.; Nakamura H. *Am. J. Clin. Nutr.* **1997**, *66*, 261. (g) Leake, D. S. In. *Flavonoids in Health and Disease*; Rice-Evans, C., Packer, L., Eds.; Marcel Dekker: New York, 1997; pp 253−276. (h) Cren-Olivé, C.; Tessier, E.; Duriez, P.; Rolando, C. *Free Radical Biol. Med.* In press.

(12) (a) Cao, Y.; Cao, R. *Nature* **1999**, *398*, 381. (b) Jankun, J.; Selman, S. H.; Swiercz, R.; Skrypczak-Jankun, E. *Nature* **1997**, *387*, 561. (c) Asano, Y.; Okamura, S.; Ogo, T.; Eto, T.; Otsuka, T.; Niho, Y. *Life Sci.* **1997**, *60*, 135. (d) Otsuka, T.; Ogo, T.; Eto, T.; Asano, Y.; Suganima, M.; Niho, Y. *Life Sci.* **1998**, *63*, 1397. (e) Chen, Z. P.; Schell, J. B., Ho, C. T.; Chen K. Y. *Cancer Lett.* **1998**, *129*, 173. (f) Liao, S.; Umekita, Y.; Guo, J.; Kokontis, J. M.; Hiipakka, R. A. *Cancer Lett.* **1995**, *96*, 239. (g) Valcic, S.; Timmermann, B. N.; Alberts, D. S.; Wächter, G. A.; Krutzsch, M.; Wymer, J.; Guillen, J. M. *Anti-Cancer Drugs* **1996**, *7*, 461. (h) Vergote, D.; Cren-Olivé, C.; Chopin, V.; Toillon, R. A.; Rolando, C.; Hondermarck, H.; Le Bourhis, X. *Breast Cancer Res. Treat.*, in press.

(13) (a) Lee, M. J.; Wang, Z. Y.; Li, H.; Chen, L.; Sun, Y.; Gobbo, S.; Balentine, D. A.; Yang, C. S. *Cancer Epidemiol., Biomarkers, Prev.* **1995**, *4*, 393. (b) Unno, T.; Takeo, T. *Biosci. Biotechnol. Biochem.* **1995**, *59*, 1558. (c) Chen, L.; Lee, M. J.; Li, H.; Yang, C. S. *Drug Metab. Dispos.* **1997**, *25*, 1045. (d) Nakagawa, K.; Miyazawa, T. *J. Nutr. Sci. Vitaminol.* **1997**, 43, 679. (e) Nakagawa, K.; Okuda, S.; Miyazawa, T. *Biosci. Biotech. Biochem.* **1997**, *61*, 1981. (f) Donavan, J. L.; Bell, J. R.; Kasim-Karakas, S.; German, J. B.; Walzem, R. L.; Hansen, R. J.; Waterhouse, A. L. *J. Nutr.* **1999**, *129*, 1662.

(14) (a) Kashima, M. *Chem. Pharm. Bull.* **1999**, *47*, 279. (b) Hanasaki, Y.; Ogawa S.; Fukui S. *Free Radical Biol. Med.* **1994**, *16*, 845. (c) Salah, N.; Miller, N. J.; Paganga, G.; Tijburg, L.; Bolwell, G. P.; Rice-Evans, C. *Arch. Biochem. Biophys.* **1995**, *322*, 339. (d) Rice-Evans, C. *Biochem. Soc. Symp.* **1994**, *61*, 103. (e) Vinson, J. A.; Hontz, B. A. *J. Agric. Food Chem.* **1995**, *43*, 401. (f) Nakao, M.; Takio, S.; Ono, K. *Phytochemistry* **1998**, *49*, 2379.

(15) Suzuki, N.; Goto, A.; Oguni, I.; Mashiko, S.; Nomoto, T. *Chem. Express* **1991**, *6*, 655.

(16) (a) Steenken, S.; Neta, P. *J. Phys. Chem.* **1982**, *86*, 3661. (b) Jovanovic, S. V.; Steenken, S.; Tosic, M.; Marjanovic, B.; Simic, M. G. *J. Am. Chem. Soc.* **1994**, *116*, 4846. (c) Jovanovic, S. V.; Hara, Y.; Steenken, S.; Simic, M. G. *J. Am. Chem. Soc.* **1995**, *117*, 9881. (d) Jovanovic, S. V.; Steenken, S.; Hara, Y.; Simic, M. G. *J. Chem. Soc., Perkin Trans. 2* **1996**, 2497. (e) Jovanovic, S. V.; Steenken, S.; Simic, M. G.; Hara, Y. In *Flavonoids in Health and Disease*; Rice-Evans, C., Packer, L., Eds.; Marcel Dekker: New York; 1997; pp 137−161. (f) Bors, W.; Saran, M. *Free Radical Res. Commun.* **1987**, *2*, 289. (g) Bors, W.; Heller, W.; Michel, C. In *Flavonoïds in Health and Disease*; Rice-Evans, C., Packer, L., Eds.; Marcel Dekker: New York; 1997; pp 111−136. (h) Bors, W.; Michel, C. *Free Radical Biol. Med.* **1999**, *27*, 1413. (i) Bors, W.; Michel, C.; Schikora, S. *Free Radical Biol. Med.* **1995**, *19*, 45. (j) Bors, W.; Michel, C.; Stettmaier, K. *Arch. Biochem. Biophys.* **2000**, *374*, 347.

(17) (a) Hirose, Y. *J. Jpn. Oil Chem. Soc.* **1998**, *47*, 509. (b) Hirose, Y.; Fujita, T.; Shima, S.; Nakayama, M. *J. Jpn. Oil Chem. Soc.* **1995**, *44*, 491. (c) Hirose, Y.; Yamaoka, H.; Akashi, H.; Nozaki, H.; Fujita, T.; Nakayama M. *Chem. Lett.* **1992**, 2361. (d) Hirose, Y.; Yamaoka, H.; Nakayama, M. *J. Am. Oil Chem. Soc.* **1991**, *68*, 131. (e) Hirose, Y.; Yamaoka; H.; Nakayama; M. *J. Jpn. Oil Chem. Soc.* **1990**, *39*, 967. (f) Hirose, Y.; Yamaoka, H.; Nakayama, M. *Agric. Biol. Chem.* **1990**, *54*, 567. (g) Valvic, S.; Burr, J. A.; Timmermann, B. N.; Liebler, D. C. *Chem. Res. Toxicol.* **2000**, *13*, 801. (h) Valvic, S.; Muders, A.; Jacobsen, N. E.; Liebler, D. C.; Timmermann, B. N. *Chem. Res. Toxicol.* **1999**, *12*, 382. (i) Sawai, Y.; Sakata, K. *J. Agric. Food Chem.* **1998**, *46*, 111−114. (j) Kondo, K.; Kurihara, M.; Miyata, N.; Suzuki, T.; Toyoda, M. *Arch. Biochem. Biophys.* **1999**, *362*, 79. (k) Kondo, K.; Kurihara, M.; Miyata, N.; Suzuki, T.; Toyoda, M. *Free Radical Biol. Med.* **1999**, *27*, 855. (l) Dangles, O.; Fargeix, G.; Dufour, C. *J. Chem. Soc., Perkin Trans. 2* **2000**, 1653.

(18) Hodnick, W. F.; Milosavljevic, E. B.; Nelson, J. H.; Pardini, R. S. *Biochem. Pharmacol.* **1988**, *37*, 2607.

(19) (a) Slabbert, N. P. *Tetrahedron* **1977**, *33*, 821. (b) Kennedy, J. A.; Munro, M. H. G.; Powell, H. K. J.; Porter, L. J.; Foo, Y. *Aust. J. Chem.* **1984**, *38*, 885. (c) Cren-Olivé, C.; Wieruszeski, J. M.; Maes, E.; Rolando, C. *Tetrahedron Lett.* **2002**, *43*, 4545.

(20) Hapiot, P.; Pinson, J.; Francesch, C.; Mhamdi, F.; Rolando, C.; Schneider, S. *J. Electroanal. Chem* **1992**, *327*, 331.

(21) (a) Hapiot, P.; Neudeck, A.; Pinson, J.; Fulcrand, H.; Neta, P.; Rolando, C. *J. Electroanal. Chem.* **1996**, *405*, 169. (b) Hapiot, P.; Pinson, J.; Neta, P.; Francesch, C.; Mhamdi, F.; Rolando, C.; Schneider, S. *Phytochemistry* **1994**, *36*, 1013. (c) Hapiot, P.; Pinson, J.; Francesch, C.; Mhamdi, F.; Rolando, C.; Neta, P. *J. Phys. Chem.* **1994**, *98*, 2641. (d) Hapiot, P.; Neta, P.; Pinson, J.; Rolando, C.; Schneider, S. *New. J. Chem.* **1993**, *17*, 211.

(22) Charton, M. *Prog. Phys. Org. Chem.* **1971**, *8*, 235−305.

Chart 1. Structures of Catechin (**I**) and of Selectively Protected Analogues[25]

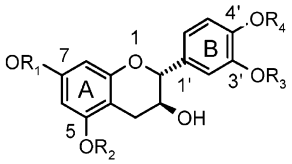

Flavan-3-ol derivatives	R1	R2	R3	R4
I	H	H	H	H
II	Me	Me	H	H
III	H	H	Me	Me
IV	H	H	C-(Ph)$_2$	
V	Me	Me	Me	H
VI	Me	Me	H	Me
VII	H	Me	C-(Ph)$_2$	
VIII	Me	H	C-(Ph)$_2$	
IX	H	H	Me	H
X	H	H	H	Me

methoxy groups correspond to slope breaking in Hammett correlations.[23] The difficulty for estimating the variation of properties from vacuum to water affects also the calculation[24] made by ab initio (mainly density functional theory (DFT)) or semiempirical calculation.

Therefore, the only solution for determining the intrinsic reactivity of each catechin moiety and for getting precise values is to use model compounds. In this study, we investigated, on one hand, the free radical chemistry of flavan-3-ols and established the structure of phenoxyl radicals by flash photolysis experiments using selectively protected catechins having either only one free phenoxy group or a ring completely protected and the other free (Chart 1). On the other hand, we obtained on these compounds experimental data: pK_a determined by NMR and $E°$ determined by cyclic voltammetry.

Materials and Methods

A. Chemicals. 3′-Methylcatechin, 4′-methylcatechin, 3′,4′-dimethylcatechin, 5,7-dimethylcatechin, 3′,5,7-trimethylcatechin, 4′,5,7-trimethylcatechin, and the different protected catechins were prepared according to the procedures developed in the laboratory and are analytically pure (microanalysis, ^{1}H and ^{13}C NMR).[25] (+)-Catechin and 5-methoxyresorcinol were commercially available (Sigma, L'Isle d'Abeau Chesnes, France) and used as received; 4-methylcatechol (Sigma, L'Isle d'Abeau Chesnes, France) was sublimed before use. The supporting electrolyte (NEt_4BF_4 or NBu_4BF_4) and the base NMe_4-$OH{\cdot}5H_2O$ (puriss) were from Fluka company (L'Isle d'Abeau Chesnes, France). Acetonitrile (ACN) was UVASOL quality (Merck, Fontenay-sous-Bois, France) and was used as received.

B. Laser Flash Photolysis Experiments. The equipment and experimental procedures have been thoroughly described in earlier papers from this laboratory.[26] Irradiations were performed with a Questek (Billerica, MA) laser 2048 (100−150 mJ/20−50 ns) using a XeCl mixture ($\lambda = 308$ nm). The detection system consisted of a 150 W xenon lamp, a 0.5 cm optical path length irradiation cell, an ARC SP 150 spectrograph (Acton Research Corp., Acto, MA), and an intensified diode array system (PG200 pulsed generator, ST-121 controller and IRY-700 S/RB detector from Princeton Instruments, Inc, Princeton, NJ). For the acquisition, the pulse width was set to 100 ns, and the delay after the laser pulse was adjusted to be as short as possible to avoid the observation of laser flash. Spectra were averaged to improve the signal-to-noise ratio.

For H-abstraction experiments, *tert*-butoxyl radicals were generated by 308 nm laser flash photolysis of 0.83 M di-*tert*-butylperoxide solutions. This concentration gave an OD $\approx$ 0.5 at the laser wavelength in the 5 mm Suprasil quartz cell. All solutions of peroxide and flavan-3-ols (10^{-3} M) were deoxygenated by purging with argon prior to the experiment. For kinetic measurements, the signals were captured by a Tektronix (Beaverton, OR) 2432 digital scope interfaced to a computer that provided suitable processing facilities. The pseudo-first-order rate constants ($k^{ap}_{PhOH/tBuO}$) were determined at 298 $\pm$ 2 K using growth curves. Absolute second-order rate constants ($k_{PhOH/tBuO}$) were calculated by least-squares fitting of plots $k^{ap}_{PhOH/tBuO}$ vs [PhOH] for at least four different concentrations of flavan-3-ols.

For direct photooxidation, phenoxyl radicals were generated directly by 308 nm laser flash photolysis of solutions of the corresponding phenolates. The concentration of the different phenolates ($(1-5) \times 10^{-4}$ M) was chosen to give an OD $\approx$ 0.5 at laser wavelength in the 5 mm Suprasil quartz cell. Special precautions were taken in the preparation of alkaline solution as solutions of basic flavan-3-ols are not stable under air: all solutions of flavan-3-ols were deoxygenated by purging with argon prior to the addition of the appropriate equivalent (one-half or one) of tetramethylammonium hydroxide 0.1 M (also deoxygenated) to form the phenolate.

C. Electrochemical Experiments. All the cyclic voltammetry were carried out at 20 $\pm$ 0.1 °C using a cell equipped with a jacket allowing circulation of water from the thermostat. The counter electrode was a Pt wire and the reference electrode an aqueous saturated calomel electrode ($E°$(SCE) = $E°$(SHE) − 0.2412 V) with a salt bridge containing the supporting electrode. The SCE electrode was checked against the ferrocene/ferrocenium couple ($E° = +0.405$ V (SCE)) before and after each experiment.

For low scan rate cyclic voltammetry (0.05−500 V s^{-1}), the working electrode was either a glassy carbon disk (3 mm diameter Tokai Carbon Corp., Tokyo, Japan) or 1 mm diameter gold disk. They were carefully polished before each voltammogram with 1 μm diamond paste and ultrasonically rinsed in absolute ethanol. Electrochemical instrumentation consisted of a PAR (Princeton Instruments) Model 175 Universal programmer and a purpose-built potentiostat equipped with a positive feed-back compensation deviced.[27] The data were acquired with a Nicolet 310 (Madison, WI) oscilloscope.

For high scan rate cyclic voltammetry, the ultramicroelectrode was a gold wire (10 μm diameter) sealed in soft glass.[28] The signal generator was a Hewlett-Packard 3314A (Palo Alto, CA) and the curves were recorded with a Nicolet 4094C (Madison, WI) oscilloscope using a minimum acquisition time of 5 ns/point. The values of the dimerization rate constants were obtained by comparison of the experimental voltammograms with simulated curves at several scan rates. The

(23) (a) Arnett, E. M.; Small, L. E.; Oancea, D.; Johnston, D. *J. Am. Chem. Soc.* **1976**, *98*, 244. (b) Fujio, M.; McIver, R. T., Jr.; Taft, R. W. *J. Am. Chem. Soc.* **1981**, *103*, 4017. (c) Anderson, P. D. J.; Fenandez, M. T.; Pocsfalvi, G.; Mason, R. S. *J. Chem. Soc., Perkin Trans. 2* **1997**, 873. (d) Hogg, J. S.; Lohmann, D. H.; Russell, K. E. *Can. J. Chem.* **1961**, *39*, 1588.
(24) (a) Karaman, R.; Huang, J. T. L.; Fry, J. L. *J. Org. Chem.* **1991**, *56*, 188. (b) McKelvey, J. M.; Alexandratos, S.; Streitwieser, A., Jr.; Abboud, J. L. M.; Hehre, W. J. *J. Am. Chem. Soc.* **1976**, *98*, 244.
(25) Cren-Olivé, C.; Lebrun, S.; Rolando, C. *J. Chem. Soc., Perkin Trans. 1* **2002**, *6*, 821.
(26) Bellec, N.; Boubekeur, K.; Carlier, R.; Hapiot, P.; Lorcy, D., Tallec, A. *J. Phys. Chem. A* **2000**, *104*, 9750.
(27) Garreau, D.; Savéant, J. M. *J. Electroanal. Chem.* **1972**, *35*, 309.
(28) Andrieux, C. P.; Garreau, D.; Hapiot, P.; Pinson, J.; Savéant, J. M. *Electroanal. Chem.* **1988**, *243*, 321.

simulated voltammograms for the radical−radical coupling mechanism were calculated by numerical resolution of the relevant set of equations according to an explicit finite difference procedure.[29] Butler−Volmer law was considered for the electron-transfer kinetics (see text). The coefficient, *R*, was taken as 0.5, and the diffusion coefficients were assumed to be equal for the all species ($D = 1.4 \times 10^{-5}$ cm^2 s^{-1}).

Solutions were purged with argon before the measurements, and argon was allowed to flow under the solution during the measurements. The concentration of flavan-3-ols was $\sim 10^{-3}$ M; the supporting electrolyte was tetrabutylammonium hexafluorophosphate (0.1 M).

D. Methodology for Quantum Chemical Calculation. The calculations were performed using the Gaussian 98 package[30a] for density functional calculations. Gas-phase geometries and electronic energies were calculated by full optimization without imposed symmetry of the conformations using the B3LYP[30b] density functional with the 6-31G* basis set,[30c] starting from preliminary optimizations performed with semiempirical methods. Because of the difficulty of running frequency calculations with the large investigated molecules, the quality of the obtained minima was checked by restarting the optimizations from other conformations, which led to the same optimized geometries.

Results

A. Free Radical Chemistry. To improve the knowledge of the mechanism of the antioxidative action of catechin and its derivatives, the free radical chemistry of flavan-3-ols was investigated. This kind of study requires appropriate models which preserve the skeleton of these polyphenols and allow the determination of the reactivity of each ring. Simple models for A and B rings, for example, 5-methoxyresorcinol, methyl gallate, and 4-methyl catechol, even if they appear very useful and more tractable to analytical methods, are not sufficient to understand all the phenomenon.[16c,d,31] The synthesis of selectively protected catechins afforded more complex models preserving the reactivity of the parent compounds (Chart 1).[25] Analogue **II** of catechin **I** is an appropriate model for B-ring study, while compounds **III** and **IV** can be used for the investigation of the A-ring reactivity. Four other compounds **V**−**VIII** allow the precise determination of the reactivity of each phenolic function since they have only one free phenoxy group. Finally the two last monomethylated derivatives **IX**, **X** are the major metabolites found in human plasma after ingestion of catechin[13,32] and thus will be particularly precious for studying the antioxidative properties not only of the native forms but also of the metabolites by flash photolysis.

We chose flash photolysis[16] for the photochemical generation of radicals and their characterization through the monitoring of their UV−visible spectra. Two different ways for generating phenoxyl radicals have been used: (i) direct photoionization of the polyphenol derivatives under their basic form and (ii) H-atom abstraction from phenolic OH by *tert*-butoxyl radicals generated by the photoionization of the di-*tert*-butylperoxide in aprotic media.

Table 1. Spectral Characteristic of Phenoxyl Radicals Generated by Photooxidation and H-Abstraction[a]

compd	ring model	photooxidation on phenolate λ_{max} (nm)	H-abstraction on phenol λ_{max} (nm)	H-abstraction on phenol ϵ (mol^{-1} L^{-1} cm^{-1})
5-methoxyresorcinol	A	495/550	495	3500
III	A	495/550	495	2700
IV	A	495/550	495	2100
VII	A	495	495	2200
II	B	380	380	6600
4-methylcatechol	B	380	380	4000
catechin **I**		380	380/495	−
3′-methylcatechin **IX**		380/495	380/495	−
4′-methylcatechin **X**		495	495	2300

[a] Delay after laser pulse respectively: 200 ns, 2 μs.

1. Characterization and Identification of Phenoxyl Radicals on Model Compounds. The identification of the radicals formed in these two experiments is readily deduced from their spectral properties (Table 1). Indeed, the comparison of the UV−vis spectra of the different model compounds allows the determination of the reaction site (Figures 1 and 2). The analogy of structure between 5-methoxyresorcinol and protected B-ring catechins **III**, **IV**, and **VII** suggests that absorption appearing at $\lambda = 495$ nm in H-abstraction (Figure 1, Table 1) and direct photooxidation (Figure 2, Table 1) experiments arises from the *m*-diphenol system, confirming previous work.[16a,c] The presence of an absorbency at $\lambda = 380$ nm in the UV spectra of 4-methylcatechol and 5,7-dimethylcatechin (**II**) radicals obtained as well as in photooxidation (Figure 2) and H-abstraction (Figure 1) experiments allows us to identify this absorbency as a characteristic of the B-ring, e.g., of the *o*-diphenol system.[16a,c] So, catechol-like phenoxyl radicals show an absorption band at 380 nm, whereas resorcinol-like phenoxyl radicals present an absorption at 495 nm.

In fact, in the case of photooxidation experiments, the spectrum of 5-methoxyresorcinol and catechins **III** and **IV** (Table 1) is more complex and presents two absorbencies in the 500 nm region: one, $\lambda_{max} = 495$ nm, which first appears 200 ns after the laser pulse while at 400 ns, the maximum of the peak moves to 550 nm. Such a red shift, which indicates a greater extent of conjugation in the final product, can reflect an acidic−basic equilibrium: after the one-electron transfer of phenolate, the resorcinol-like phenoxyl radical loses, in a basic medium, a proton to become a radical anion,[33] whose UV characteristic peak is an absorption band at 550 nm. Moreover, during the photooxidation of the B-ring protected compound **VII**, which has only one free hydroxyphenyl function, only the absorbency at 495 nm was expected and detected. In the case of catechol-like models only the radical anion is observed as shown by Simic et al.[16d]

2. Reactivity of Catechin and Its Monomethylated Metabolites. Catechin exhibited a more complex behavior. H-

(29) Amatore, C.; Garreau, D.; Hammi, M.; Pinson, J.; Savéant, J. M. *Electroanal. Chem.* **1985**, *184*, 1.
(30) (a) Frisch, M. J.; Trucks, G. W.; Schlegel, H. B.; Scuseria, G. E.; Robb, M. A.; Cheeseman, J. R.; Zakrzewski, V. G.; Montgomery, J. A.; Stratmann, R. E.; Burant, J. C.; Dapprich, S.; Millam, J. M.; Daniels, A. D.; Kudin, K. N.; Strain, M. C.; Farkas, O.; Tomasi, J.; Barone, V.; Cossi, M.; Cammi, R.; Mennucci, B.; Pomelli, C.; Adamo, C.; Clifford, S.; Ochterski, J.; Petersson, G. A.; Ayala, P. Y.; Cui, Q.; Morokuma, K.; Malick, D. K.; Rabuck, A. D.; Raghavachari, K.; Foresman, J. B.; Cioslowski, J.; Ortiz, J. V.; Stefanov, B. B.; Liu, G.; Liashenko, A.; Piskorz, P.; Komaromi, I.; Gomperts, R.; Martin, R. L.; Fox, D. J.; Keith, T.; Al-Laham, M. A.; Peng, C. Y.; Nanayakkara, A.; Gonzalez, C.; Challacombe, M.; Gill, P. M. W.; Johnson, B. G.; Chen, W.; Wong, M. W.; Andres, J. L.; Head-Gordon, M.; Replogle, E. S.; Pople, J. A. *Gaussian 98* (Revision A.1); Gaussian, Inc.: Pittsburgh, PA, 1998. (b) Becke, A. D. *J. Chem. Phys.* **1993**, 98, 5648.
(31) Cren-Olivé, C.; Lebrun, S.; Hapiot, P.; Pinson, J.; Rolando, C. *Tetrahedron Lett.* **2000**, *41*, 5847.
(32) (a) Ho, Y.; Lee, Y. L.; Hsu, K. Y. *J. Chromatogr. B* **1995**, *665*, 383. (b) Bell, J. R. C.; Donavan, J. L.; Wong, R.; Waterhouse, A. L.; German, J. B.; Walzem, R. L.; Kasim-Karakas, S. *Am. J. Clin. Nutr.* **2000**, *71*, 103. (c) Harada, M.; Kan, Y.; Naoki, H.; Fukui, Y.; Kageyama, N.; Nakai, M.; Miki, W.; Kiso, Y. *Biosci., Biotechnol., Biochem.* **1999**, *63*, 973. (d) Li, C.; Lee, M. J.; Sheng, S.; Meng, X.; Prabhu, S.; Winnik, B.; Huang, B.; Chung, J. Y.; Yan, S.; Ho, C. T.; Yang, C. S. *Chem. Res. Toxicol.* **2000**, *13*, 177.
(33) (a) Steenken, S.; Neta, P. *J. Phys. Chem.* **1979**, *83*, 1134. (b) Steenken, S.; O'Neill, P. *J. Phys. Chem.* **1977**, *81*, 505.

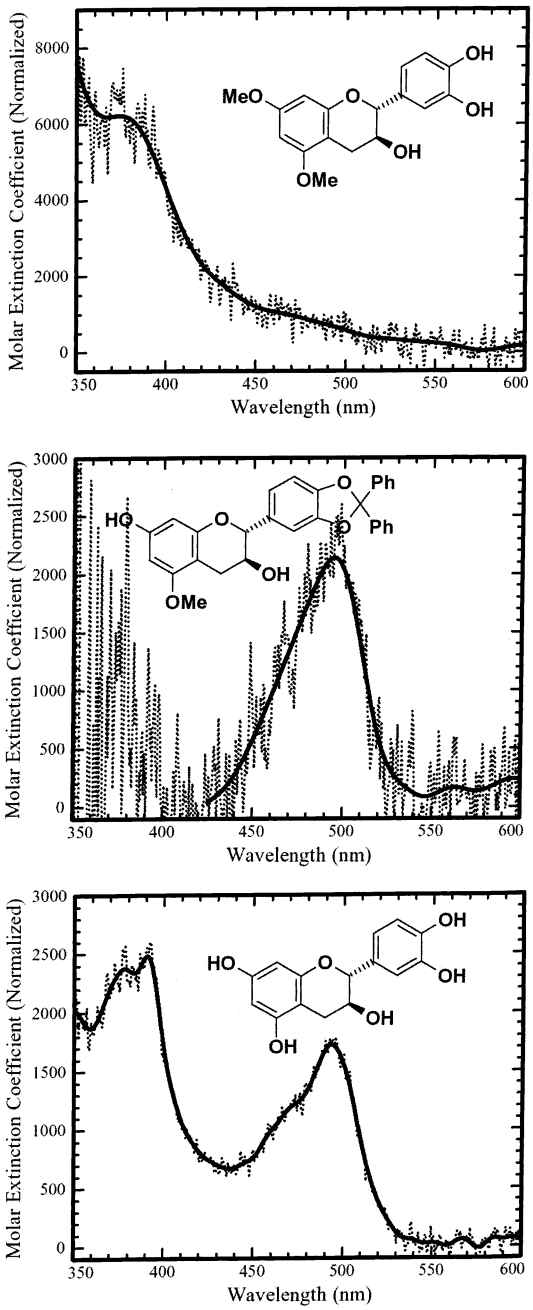

Figure 1. UV−vis spectra of catechin (lower panel) and its analogues **II** (upper panel) and **VII** (middle panel) phenoxyl radicals obtained by H-abstraction experiments (solution of 8.27×10^{-1} M of di-*tert*-butylperoxide and 3.21×10^{-3} M of catechin in acetonitrile, and respectively of **II** or **VII** (average of five spectra; time after pulse, 2 μs). Curves were obtained by high-frequency filtering of experimental data displayed by dots on the graphs.

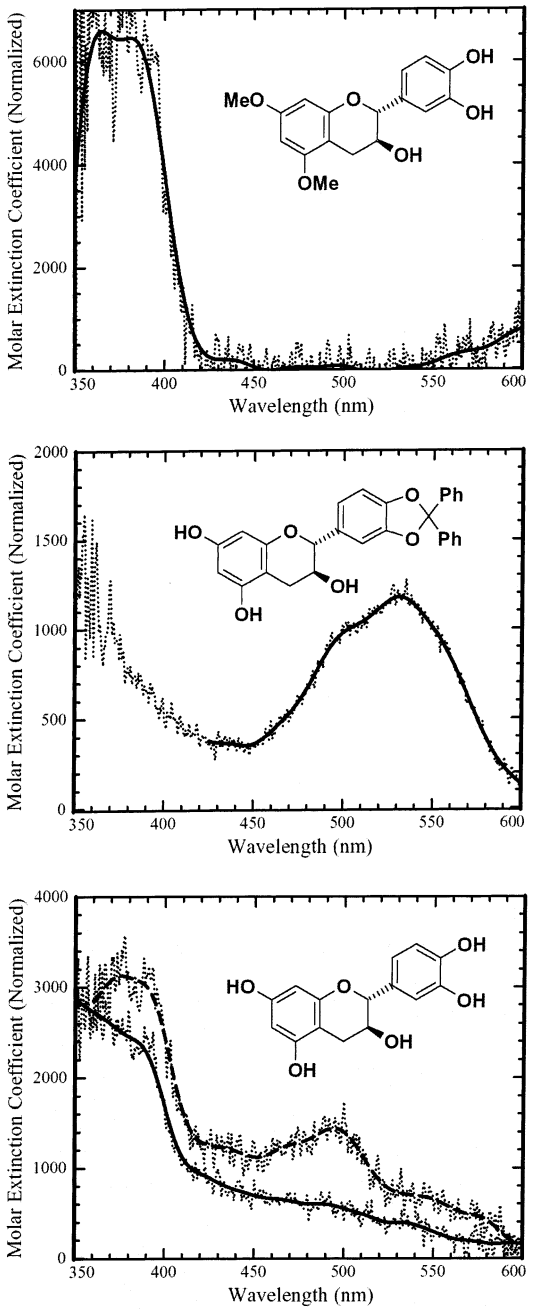

Figure 2. UV−vis spectra of phenoxyl radical obtained upon direct irradiation in acetonitrile of (lower panel) catechin phenolate (solution of 2.55×10^{-4} M of catechin with 1 equiv of tetramethylammonium hydroxide (0.1 M; dashed line) or solution of 4.28×10^{-4} M of catechin with 1/2 equiv (unbroken line) of base); (upper panel) catechin analogue **II** phenolate (solution of 6.16×10^{-4} M of **II** with 1 equiv of base) and (middle panel) catechin analogue **IV** phenolate (solution of 9.42×10^{-4} M of **IV** with 1 equiv of base). Average of 10 spectra; time after pulse, 200 ns. Curves were obtained by high-frequency filtering of experimental data displayed by dots on the graphs.

abstraction on catechin by *tert*-butoxyl radicals gave a spectrum characterized by two absorption bands respectively at $\lambda = 380$ and 495 nm (Figure 1). The 308 nm laser-induced photooxidation of catechin phenolate in the presence of 1 equiv of base produced a similar spectrum ($\lambda = 380$ and 495 nm), whereas in the presence of 1/2 equiv of base only one absorption band at $\lambda = 380$ nm was obtained (Figure 2).

The comparison with the spectra obtained for the model compounds allows the precise identification of the phenoxyl radicals formed upon photooxidation and H-abstraction (Figures 1 and 2). So H-abstraction of catechin leads to two different radicals: an A-ring resorcinol-like phenoxyl radical characterized by an absorption band at $\lambda = 495$ nm and a B-ring catechol one absorbing at $\lambda = 380$ nm (Scheme 1). A more precise inspection of the absorbencies shows, however, that the H-abstraction is a selective process since 70% of the reactivity occurs on the A-ring.

In contrast, upon photooxidation of catechin, in the presence of 1/2 equiv of base, only the catechol-like radical characterized

Scheme 1. H-Abstraction of Catechin by *tert*-Butoxyl Radicals

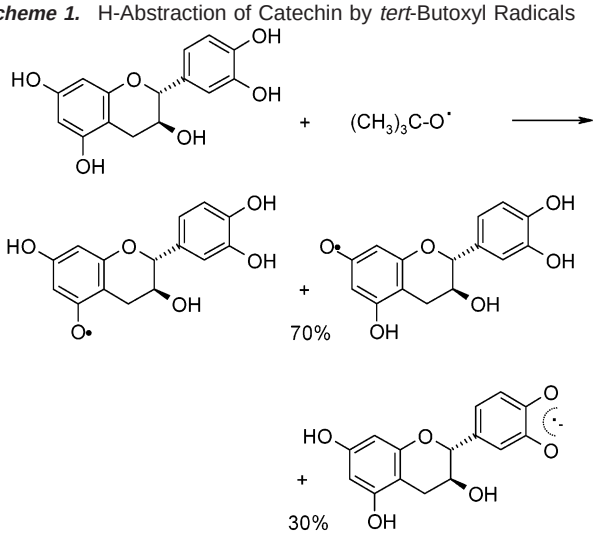

Scheme 2 Photooxidation of Catechin

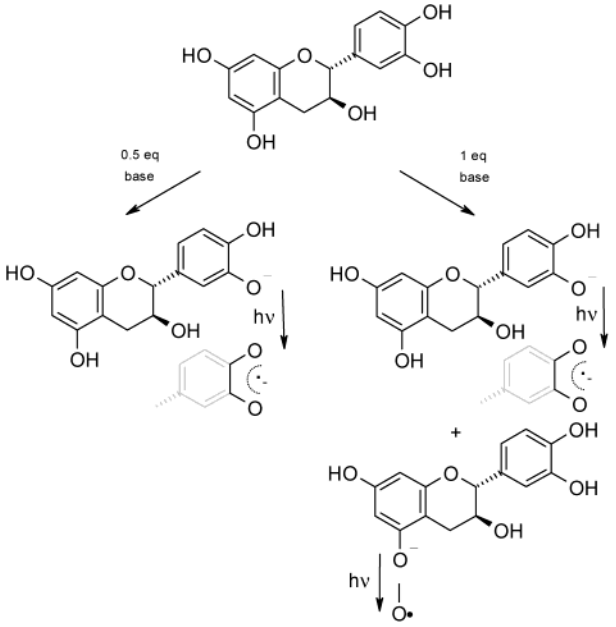

by an absorption band at $\lambda = 380$ nm appeared, while in the presence of 1 equiv of base, both resorcinol- and catechol-like radicals were formed (Scheme 2). This selectivity of direct irradiation experiments is related to the possibility of deprotonating a single or several phenolic functions since only phenolates absorb the laser light and are much more easily oxidizable than neutral phenols. So the absorption at $\lambda = 380$ nm, characteristic of a catechol-like radical, is related to the photooxidation of the first deprotonated phenolic function.

The chemical behavior of 3′-methyl- and 4′-methylcatechin is now particularly interesting to study since they are the major metabolites circulating in the plasma identified currently. The spectra obtained for these two compounds upon flash photolysis experiments are presented Figure 3. While the 308 nm laser-induced photooxidation in the presence of 1/2 equiv of base and the H-abstraction of 3′-methylcatechin led to the formation of both kinds of radicals (the resorcinol- and catechol-like radicals characterized by an absorption band at $\lambda = 495$ and 380 nm, respectively), in the case of 4′-methylcatechin, the resorcinol-like phenoxyl radical is selectively formed.

As seen before, the photooxidation experiments allow us to discuss the relative acidity of each catechin ring. The apparition of both radicals issued from each ring in equal quantity during the photooxidation of 3′-methylcatechin shows that the methylation of the 3′ position, the most acidic position in catechin, reduces the pK_a difference existing between the two rings. On the contrary, the methylation of the 4′ position changes drastically the protonation sequence of flavan-3-ols: the radical absorbing at 495 nm constitutes 84% of the mixture (Figure 3), which indicates that, in this case, the A-ring is the most acidic one. Yet, during the H-abstraction experiments of the two compounds (3′-methylcatechin and 4′-methylcatechin), only the resorcinol-like phenoxyl radical appeared. So the methylation of one of the two sites of the B-ring increases the selectivity observed on catechin.

So, this study allows the determination of the influence of the monomethylation of the B-ring on the reactivity of flavan-3-ol by comparing the results obtained on catechin and on the two monomethylated compounds. While the monomethylation of the B-ring just enhances the selectivity of the H-abstraction on the A-ring, it implies drastic changes in the behavior upon photooxidation which indicates that the physical parameters are greatly affected by the methylation.

3. H-Abstraction Kinetic Measurements. The ability of flavan-3-ols to intercept or inactivate damaging free radicals before they reach vital cell components or to chemically repair damaged biomolecules or bioradicals thus reversing damage is evaluated by H-abstraction kinetic measurements. *tert*-Butoxyl radicals were generated "instantaneously"[34] by 308 nm laser flash photolysis of di-*tert*-butylperoxide at 298 K. The catechin analogues were used in large excess relative to the *tert*-butoxyl radicals so that the hydrogen atom abstraction from catechin analogues by *tert*-butoxyl radicals could be monitored by following the pseudo-first-order growth of the 380 or 495 nm absorption of the phenoxyl radicals (Scheme 3).

Scheme 3. H-Abstraction of Flavan-3-ols

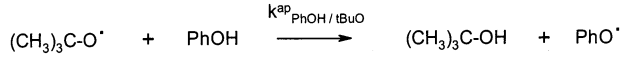

Absolute second-order rate constants $k_{PhOH/tBuO}$ were obtained by least-squares fittings plots of $k^{ap}_{PhOH/tBuO}$ vs [PhOH] according to the eq 1**,** assuming that the reverse reaction rate constant is negligible in comparison to $k_{PhOH/tBuO}$ as would be expected since all the reactions studied are exothermic. k_0 is the kinetic constant that characterized the decay of tBuO• without added catechin (self-decomposition of the radical and reaction with impurities). We assume that the reaction of tBuO• with impurities does not change much when adding catechin and between individual experiments. At least three separate measurements of $k^{ap}_{PhOH/tBuO}$ were made at each concentration of phenolic compound, and at least four different concentrations of PhOH were employed. All of these plots gave excellent straight lines ($r^2 \geq 0.98$), and values of $k_{PhOH/tBuO}$ are given in Table 2.

$$k^{ap}_{PhOH/tBuO} = k_0 + k_{PhOH/tBuO}[\text{substrat}] \qquad (1)$$

(34) Evans, C., Scaiano, J. C.; Ingold, K. U. *J. Am. Chem. Soc.* **1992**, *114*, 4589.

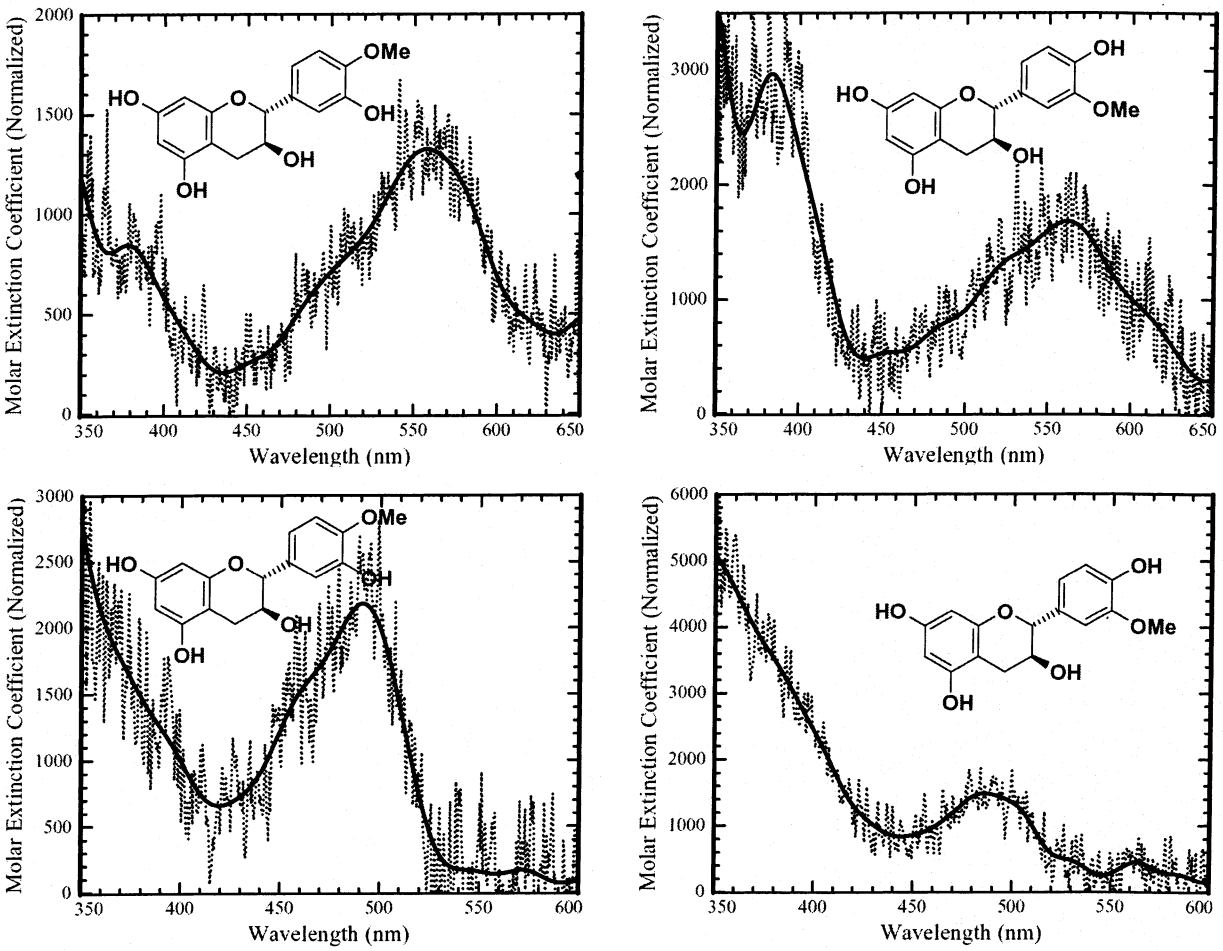

Figure 3. UV−vis spectra of 3′- and 4′-methylcatechin phenoxyl radicals obtained upon photooxidation (upper panel) in the presence of 1/2 equiv of tetramethylammonium hydroxide (0.1 M; solution of 6.0×10^{-4} M of **IX** and **X** in acetonitrile; average of three spectra; time after pulse, 200 ns) and H-abstraction experiments (lower panel; solution of 8.27×10^{-1} M of di-*tert*-butylperoxide and 9.0×10^{-4} M of **IX** and **X** in acetonitrile; average of three spectra; time after pulse, 2 μs). Curves were obtained by high-frequency filtering of experimental data displayed by dots on the graphs.

Table 2. Rate Constants ($k_{PhOH/tBuO}$) of the Reaction of H-Abstraction on Flavan-3-ols by *tert*-Butoxyl Radicals

compd	growth of the absorption at	$10^{-8}k_{PhOH/tBuO}$ (±20%)
VII	495 nm	0.8
IV	495 nm	2.3
III	495 nm	2.3
II	380 nm	1.7
catechin	495 nm	2.0
	380 nm	2.0
3′-methylcatechin **IX**	495 nm	2.3
4′-methylcatechin **X**	495 nm	2.9

So for this family of compounds, the rates of H-abstraction by *tert*-butoxyl radicals in acetonitrile, around $(1-3) \times 10^8$ M^{-1} s^{-1}, reflect their favorable antioxidant properties. More precisely, these values are very close to the rate constants obtained for H-abstraction on α-tocopherol by *tert*-butoxyl radicals in acetonitrile (6.6×10^8 M^{-1} s^{-1}),[34] indicating that, in aprotic medium, catechin and its methylated metabolites are excellent free radical scavengers, comparable to α-tocopherol.

Besides, the more precise inspection of the kinetics obtained for the two radicals formed in the case of catechin, i.e., the resorcinol ($\lambda = 495$ nm) and catechol ($\lambda = 380$ nm) like phenoxyl radicals (Figure 4) shows that the resorcinol-like radical is a short-lived transient, while the catechol-like one can be described like a long-lived phenoxyl radical, in agreement with a previous pulse-radiolytic study of Jovanovic et al.[16c] But the decay of the resorcinol-like radical absorbing at $\lambda = 495$ nm is not correlated to any increase of the signal of the catechol-like radical characterized by an absorption band at $\lambda = 380$ nm (Figure 4). So, we can conclude that the resorcinol-like radical transforms quickly to another transient which is not the catechol-like radical, contrary to the hypothesis made in the previous study.[16c] In our conditions, the inter- or intramolecular transformation of the resorcinol-like radicals into B-ring radical is not observed.

B. Electrochemistry. Flash photolysis and electrochemistry techniques afford complementary information for the study of reaction mechanisms involving electron transfer. Indeed, while flash photolysis allows, as we have just discussed, the characterization of short-lived intermediates by recording their UV spectra and the determination of the reaction kinetics starting in the low-microsecond range, electrochemistry permits first the characterization of the intermediates formed upon electronic transfer by its reduction/oxidation pattern and second the determination of the mechanism of the reaction following the first electronic transfer.

However, the electrochemical study of flavan-3-ols is a real challenge: indeed, as for phenolic derivatives[20,21,35] and a fortiori

(35) (a) Elving, P. J.; Krivis, A. F. *Anal. Chem.* **1958**, *30*, 1645. (b) Rapta, P.; Misik, V.; Stasko, A.; Vrabel, I. *Free Radical Biol. Med.* **1995**, *18*, 901.

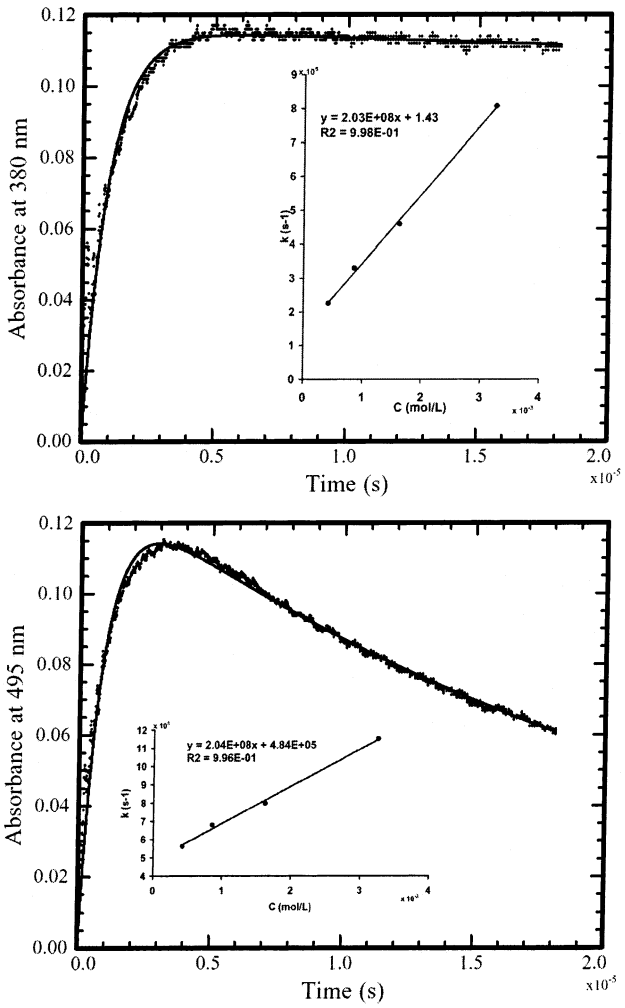

Figure 4. Growth of the catechol-like phenoxyl absorption at 380 nm (upper panel) following 308 nm laser flash photolysis of a 3.3×10^{-3} M solution of catechin in di-*tert*-butylperoxide (0.83 M). Insert: Variation in the first-order growth-in rate constant as a function of the catechin concentration. Apparition of resorcinol-like radical absorbing at $\lambda = 495$ nm (lower panel; solution of 3.3×10^{-3} M of catechin; 0.83 M of di-*tert*-butylperoxyde in acetonitrile). Insert: Variation in the first-order growth-in rate constant as a function of the catechin concentration.

polyphenolic ones,[16e,18,36] the monoelectronic oxidation of flavan-3-ols generates phenoxyl radicals which form polymeric products. This polymerization can lead to an insulating film that sticks to the electrode, hampering the accuracy of the measurements. In water, a medium in which the polymerization is faster than in aprotic solvents such as acetonitrile,[21c,35b] the electronic transfer has been shown to be slow[21d] and thus to become the determining step of the electrochemical process. This precludes the possibility of obtaining significant kinetic data for the reaction following the first electronic transfer.

Therefore, to avoid these two major drawbacks, we decided to examine, in aprotic medium, the behavior of model compounds such as **V**−**VIII**, which offer only one free hydroxyl function, first by cyclic voltammetry at low scan rate and second at fast scan rate using ultramicroelectrodes. To avoid the reactions due to the proton transfer and because the interesting redox potential for understanding biological effects of flavan-3-ols is the one related to the couple phenoxyl radical/ phenolate, it is the oxidation of the corresponding phenolates of **V**−**VIII**, obtained after addition of 1 equiv of tetramethylammonium hydroxide, that was investigated.

Table 3. Oxidation Parameters of the Flavan-3-ols in Acetonitrile

compd	position of free OH	Ep_a[a] (mV/SCE)	$\delta Ep/\delta \log(v)$[a] (mV)	k_{cons}[b] (10^{-8} M^{-1} s^{-1})	$k^{app}{}_s$[b] (cm s^{-1})
VI	3	10	40	3.5 (±1.5)	0.30
V	4	22	28	3.5 (±1.5)	0.40
VIII	5	164	19	3.5 (±1.5)	0.15
VII	7	125	40	−	−

[a] Parameters derived from cyclic voltammetry at low scan rate (see text and Experimental Section). [b] Parameters derived from cyclic voltammetry at fast scan rate (see text and Experimental Section).

1. Cyclic Voltammetry at Low Scan Rate. In acetonitrile on a glassy carbon electrode at slow scan rate ($v = 0.2$ V s^{-1}), the four phenolates **V**−**VIII** exhibit a broad irreversible oxidation peak with a peak potential $Ep_a = -0.02$, -0.01, $+0.12$, and $+0.16$ V/SCE, respectively. Typical voltammograms of the oxidation of the phenolate of **V** and **VIII** at a scan rate of 0.2 V s^{-1} are shown in Figure 5, and all results are summarized in Table 3. The peak height indicates the exchange of one electron per molecule by comparison with the intensity of the peak current of ferrocenemethanol under the same conditions. So, as we have noticed above, the peaks corresponding to the oxidation of the studied phenolates are broad and badly defined due to the polymerization process. The phenolic groups in position 3′ (compound **VI**) and 4′ (compound **V**) appear, as expected, much more oxidizable than the ones in position 5 (compound **VIII**) and 7 (compound **VII**) since the two first positions possess in ortho a methoxyl group which is an electrodonating substituent.

The interest of these experiments at low scan rate is to allow the characterization of the mechanism of the reaction following the first electronic transfer by the study of the variation of the peak potential Ep_a with the scan rate.[37] Repeated and consistent experiments (Figure 5) showed that, for phenolate **V**, the oxidation peak shifts by 28 mV/log(v) toward positive values upon raising the scan rate and for phenolate **VIII**, the slope of the variation of oxidation peak with scan rate is around 19 mV/log(v), while, for the last compounds **VI** and **VII**, the oxidation peak potential increases linearly with the logarithm of scan rate with a slope around 40 mV/log(v) (Table 3). This last situation is particularly unfavorable since it indicates a mixed control of the global kinetics, i.e., by the electron-transfer step and by a subsequent chemical reaction, so no information can be obtained on the mechanism of the subsequent reaction.[38a−c] This situation has already been found during the oxidation of ferulic or coumaric acids into phenoxonium cations in acetonitrile.[21a]

Yet, the study of the phenolates **V** and **VIII** is much more instructive for the comprehension of the reaction following the electronic transfer. In the case of compound **VIII**, which allows the study of the reactivity of the phenolic function in the 5 position, the slope of 19 mV/log(v) is consistent with a

(36) (a) Engelkemeir, D. W.; Geissman, T. A.; Crowell, W. R.; Friess, S. L. *J. Am. Chem. Soc.* **1947**, *69*, 155. (b) Geissman, T. A.; Freiss, S. L. *J. Am. Chem. Soc.* **1949**, *71*, 3893−3902.

(37) A slope of 29.1 mV per log(v) is expected for the variation of the peak potential with the scan rate for a DIM 2 mechanism (fast electron transfer followed by an irreversible phenolate−phenoxyl radical coupling) at 20 °C. A slope of 19.3 mV per log(v) is expected for the variation of the peak potential with the scan rate for a DIM 1 mechanism (fast electron transfer followed by an irreversible radical phenoxyl−phenoxyl radical coupling) at 20 °C.[38a−c]

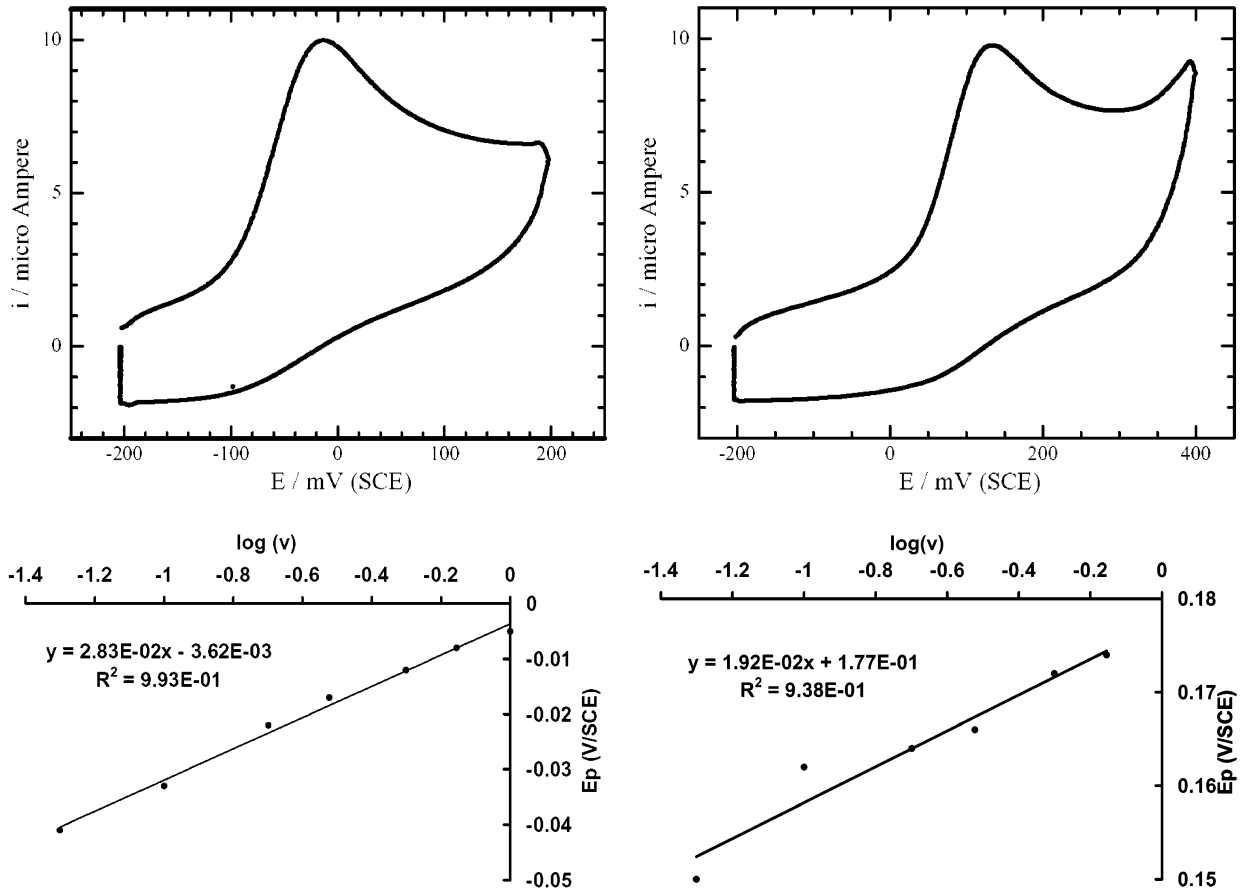

Figure 5. Cyclic voltammetry of phenolate **V** (upper and lower left panels) and phenolate **VIII** (upper and lower right panels) in acetonitrile: (upper left panel) $\upsilon = 0.2$ V s^{-1}, $C° = 1.0$ mM, 0.1 M NBu_4BF_4, 3 mm diameter glassy carbon electrode; (lower left panel) variation of the peak potential as a function of the scan rate υ; (upper right panel) $\upsilon = 0.2$ V s^{-1}, $C° = 1.0$ mM, 0.1 M NBu_4BF_4, 3 mm diameter glassy carbon electrode; (lower right panel) variation of the peak potential as a function of the scan rate υ.

Scheme 4. DIM 1 Mechanism Involved in the Dimerization of Compound **VIII**

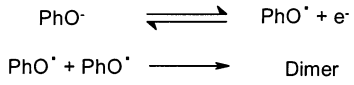

mechanism involving a fast electron transfer between the electrode and the phenolate followed by an irreversible coupling of the two radicals (DIM 1 mechanism)[38a−c] as described in Scheme 4.

The reactivity of compound **V**, offering the 4′ phenolic function free, is different since the slope of 28 mV/log(υ) obtained indicates usually a first-order consecutive reaction.[38a−c] As far as the oxidation of phenolates is concerned, the behavior observed points to the occurrence of a DIM 2 mechanism which consists of a fast electron transfer followed by the coupling of a phenoxyl radical with an excess phenolate to give a dimer radical anion. This species can be immediately oxidized at the electrode surface and/or by electron exchange with a radical phenoxyl (Scheme 5). Similar results were obtained for protected analogues of coniferyl alcohol like 2,6-dimethyl-4-(3-hydroxy-3-methyl-1-butyl)phenol and 2,6-dimethyl-4-(3-hydroxy-3-methyl-1-butynyl)phenol, where the coupling between a phenoxyl radical with the phenolate was found to be the key step in the formation of the dimer.[21d]

Scheme 5. DIM 2 Mechanism Involved in the Dimerization of Compound **V**

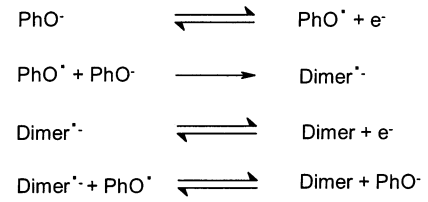

2. Cyclic Voltammetry at Fast Scan Rate. The use of ultramicroelectrodes in acetonitrile permits one to reach very high scan rates. It is then possible to observe that the electronic transfer becomes reversible upon raising the scan rate up to values in the 10 000 V s^{-1} range. Figure 6 shows typical examples of cyclic voltammograms obtained under such conditions for phenolates **V** and **VIII.** These results indicate that the phenoxyl radicals are detectable on this time scale: we can note that the return wave is quite large due to a slow electron transfer. The standard potential of the phenoxyl radical/phenolate redox couples can be immediately derived from such experiments as the midpoint between the anodic and cathodic peak potentials for the different phenolates (Table 4). The catechol B-ring ($E°_{OH_{3'}} = 0.135$ V/SCE, $E°_{OH_{4'}} = 0.110$ V/SCE) is, as expected, more oxidizable than the resorcinol A-ring ($E°_{OH_5} = 0.285$

(38) (a) Nadjo, L.; Savéant, J. M. *Electroanal. Chem. Interfacial Electrochem.* **1973**, *48*, 113. (b) Andrieux, C. P.; Savéant, J. M. In *Investigations of Rates and Mechanisms of Reactions*; Bernasconi C. F. Ed.; John Wiley & Sons: New York, 1986; Vol. 6, A/E, Part 2, pp 305−390. (c) Andrieux, C. P.; Nadjo, L.; Savéant, J. M. *Electroanal. Chem. Interfacial Electrochem.* **1973**, *42*, 223. (d) Richards, J. A.; Whitson, P. E.; Evans, D. H. *J. Electroanal. Chem.* **1975**, *63*, 311.

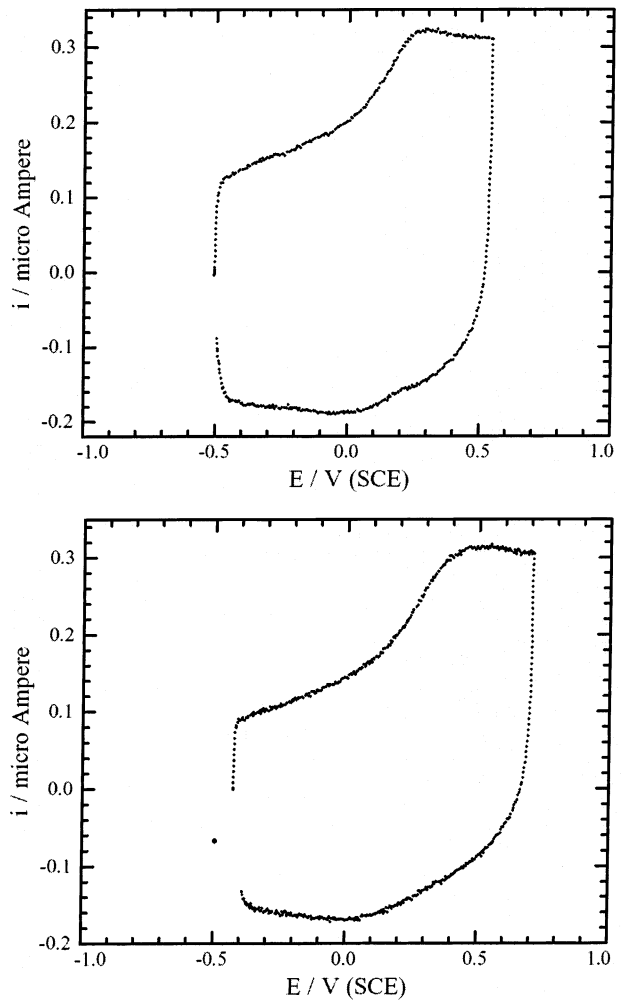

Figure 6. Cyclic voltammetry in acetonitrile of phenolate **V** (upper panel, $v = 11\ 500$ V s^{-1}, $C° = 1.8$ mM, 0.1 M NEt_4BF_4, 10 μm platinum diameter ultra-microelectrode) and phenolate **VIII** (lower panel, $v = 11\ 500$ V s^{-1}, $C° = 2.0$ mM, 0.1 M NEt_4BF_4, 10 μm platinum diameter ultra-microelectrode).

Table 4. Standard Potentials of Flavan-3-ols in Acetonitrile Obtained by Cyclic Voltammetry at Fast Scan Rate

compd	$E°$ (V/SCE)	compd	$E°$ (V/SCE)
V	0.110	**VII**	–
VI	0.135	**VIII**	0.285

V/SCE), and on the B-ring, the more oxidizable phenolic function is the more basic site.

The values of the standard electron-transfer rate constants k^{app}_s are derived from the difference between the anodic and cathodic peaks assuming that $\alpha = 0.5$ and taking for the diffusion coefficient D the value found for the 2,4,6-tri-*tert*-butylphenolate (1.4×10^{-5} cm^2 s^{-1}).[38d] The transition between the irreversible behavior observed at low scan rates and the reversible behavior at high scan rates was used to derive the rate constants for the consecutive reaction. More precisely, the values of the dimerization rate constants were obtained by comparing the experimental voltammograms with simulated curves for the radical−radical coupling mechanism (see Experimental Section).[29] The results obtained for k^{app}_s and k_{cons} are summarized with other data in Table 3. From these values, it is noticeable that the dimerization or dismutation of phenoxyl radicals is very fast with a rate constant close to 10^8 M^{-1} s^{-1}.

Table 5. B3LYP Electronic Energy, E^{elec}, of the Catechin Phenoxyl Radicals and Calculated Bond Dissociation Enthalpy (BDE) for Each Phenolic Function

bond	$E_{phenoxyl\ radical}$ (hartrees)	BDE[a] (kcal/mol)
4′ O−H	1030.709 238	75.1
3′ O−H	1030.708 239	75.8
5 O−H	1030.695 113	84.0
7 O−H	1030.693 418	85.0

[a] BDE estimated as $E^{elec}_{phenoxyl\ radical} + E^{elec}_{H-atom} - E^{elect}_{catechin} + RT$. Electronic energy of catechin = −1031.328 852 hartrees and H-atom electronic energy = −0.500 272 hartree.

The values obtained for all the studied compounds are similar, so there is no selectivity as a function of the position of the phenolic function. Thus, these rates are only characteristic of the oxidation of phenolic or polyphenolic compounds since similar results were obtained also for different analogues of cinnamic alcohol, aldehyde, and acids.[20,21]

C. Theoretical Modeling. To rationalize the observed behaviors, we performed a series of molecular modeling calculations to determine both the geometry and the stability of catechin in three states: phenol, phenolate, and phenoxyl radical. The geometries of the neutral, phenolate, and phenoxyl radical were determined by a full optimization of the conformation using the B3LYP[30b] density functional[30c] as a compromise between precision and calculation time. We made these calculations for each of the four phenolic functions of catechin 3′, 4′, 5, and 7. The typical optimized geometries calculated at the B3LYP/6-31G* level for catechin, its 4′-phenoxyl radical, and 4′-phenolate are presented in the Supporting Information as well as the calculated dihedral angle, charge, and spin distribution for all the compounds.

The geometries of all the compounds neutral, radical, and phenolate are similar: as expected, the chromane moiety appears planar and the angle between this chromane moiety and the B-ring is unchanged upon all the series of compounds whatever their oxidation and charge state ($O_1C_2C_{1'}$ angle approximately equal to 112°), suggesting that these two moieties of the molecule are independent so that delocalization of charge and spin over the whole molecular framework, as previously described,[16b] does not exist. This is supported by the examination of the charge and spin distribution of each phenolate and phenoxyl radical (see Supporting Information Table 2): unpaired electron and/or charge are located on the phenolic cycle, A or B, where the deprotonation or H-abstraction occurs.

This theoretical method also gives accurate relative energies for a family of related phenolic compounds and should give a reasonable value for the bond dissociation energy (BDE) of phenol itself. Table 5 shows the electronic energy calculated for the phenoxyl radicals of catechin obtained using the B3LYP functional. As expected, the lowest values on the B-ring are obtained when the OH group points toward the radical allowing stabilization by formation of hydrogen bonding. Given the H atom electronic energy ($E_{elec}(H) = -0.500\ 272$ hartree), and after adding RT to convert from energy to enthalpy ($H = E_{elec} + PV = E_{elec} + RT$), BDE values can be approximated by the following equation: E_{elec}(phenoxyl radical) + $E_{elec}(H)$ − E_{elec}(catechin) + RT. The final column of Table 5 shows the values of $\Delta H°_{298}$ for the reaction PhOH → PhO° + H°. These

values are in good agreement with experimental[39−41] and theoretical[42] values of BDEs of simple phenols. Indeed, the experimental value for BDE(PhO−H)$_{gas}$ is 87.3 ± 1.5 kcal/mol.[39,40] This is the mean of experimental measurements by photoacoustic calorimetry in five solvents having very different hydrogen bond accepting properties (range 86.2−88.3 kcal/mol).[40] Optimized calculations on phenol and a large number of substituted phenols give a value for BDE(PhO−H)^{gas} of 86.46 kcal/mol.[42]

Discussion

A. Structure of Flavan-3-ol Phenoxyl Radicals. The use of selectively protected catechin analogues preserving the parent reactivity allows us to reach a better understanding of the free radical chemistry of flavan-3-ols and also to rationalize the discrepancies regarding the structure of the phenoxyl radicals.[16b,c,h−j] Indeed, the two phenoxyl radicals formed upon oxidation of catechin have been characterized and identified unambiguously: the short-lived one is a resorcinol-like (A-ring) radical characterized by an absorption band at $\lambda = 495$ nm, while the second one, a long-lived transient, can be ascribed as a catechol-like (B-ring) phenoxyl radical absorbing at $\lambda = 380$ nm. These results contradict the hypothesis concerning the structure of the phenoxyl radical of a recent pulse radiolysis study[16h] but corroborate the one described by Jovanovic et al.[16b] Yet, our experiments cannot confirm the last hypothesis of the last authors,[16b] i.e., an intra- or intermolecular electron transfer from the A-ring phenoxyl radical leading to the transformation of the resorcinol-like phenoxyl radical into catechol-like radical.

B. Determination of Microscopic Dissociation Constants. In case of flavan-3-ols, even if the successive catechin pK_a values have been determined by various methods[19a,b] agreeing with first and second pK_a about 8.7 ± 0.1 and 9.4 ± 0.1 in water, neither the protonation sequence between the two rings nor the intrinsic pK_a of the four phenol groups has been clearly established. Indeed, while Slabbert[19a] proposes a BAAB sequence, Kennedy et al.[19b] prefer a deprotonation beginning on A-ring (ABAB). Our results obtained during photooxidation experiments indicate that the first pK_a of rings A and B are close: addition of 1 equiv of base gave a mixture of phenolates leading to a mixture of phenoxyl radicals after irradiation. But the selectivity observed with 1/2 equiv of base indicates that the catechol B-ring is slightly more acidic in acetonitrile. A similar order between the two rings must occur in water, as suggested by Slabbert[19a] and as the relative acidities of phenols are generally not affected by solvents effects.[43]

We have confirmed these results by a NMR study of the deprotonation of catechin affording the microscopic pK_a (Table 6).[19c] Indeed the successive deprotonations of the different phenolic functions present on flavan-3-ols induce great changes in the chemical environment of various carbons of the skeleton, reflected in the ^{13}C NMR chemical shifts.[44] More precisely, the deprotonation of a phenolic function induces deshielding for the ipso and ortho carbon atom and shielding for the para carbon atom. Such selective behavior allows, with the unambiguous assignment of ^{13}C NMR signals of flavan-3-ols, the determination of the precise deprotonation site of catechin and epicatechin.[19c] The quantification of each existing species allows the determination of the intrinsic pK_a (Table 6). The NMR studies are the only method yielding these microscopic pK_a in the case of polyphenolic compounds.

Table 6. Acid−Base Properties of Catechin

phenolic function	microscopic pK_a determined by NMR study (±0.05)	phenolic function	microscopic pK_a determined by NMR study (±0.05)
3′	9.02	5	9.43
4′	9.12	7	9.58

Table 7. Experimental and Calculated Formal Potential E°, Variations with the Radical Position in Catechin

phenoxyl radical position	exptl E° (V/SCE)	exptl ΔE° [a]	electronic energy, E^{elec}, of the phenolate (hartrees)	electronic energy, E^{elec}, of the phenoxyl radical (hartrees)	calcd ΔE° [b] (eV)
4′	0.110	0	1030.776 211	1030.709 238	0
3′	0.135	0.025	1030.776 255	1030.708 239	0.028
5	0.285	0.175	1030.767 532	1030.695 113	0.148
7	−		1030.762 459	1030.693 418	0.056

[a] $\Delta E^\circ = E^\circ - E^\circ_{4'}$. [b] ΔE° estimated as $= (E^{elec}_{radical} - E^{elec}_{phenolate}) - (E^{elec}_{radical} - E^{elec}_{phenolate})_{4'}$.

C. Determination of Standard Potential. The high scan rate cyclic voltammetry results allow us to characterize entirely the phenoxyl radicals formed upon monoelectronic oxidation of the phenolate in acetonitrile. The standard potential of each radical has been determined (Table 4), allowing access to the thermodynamic characteristic of each phenolic function present on catechin, which has never been realized until now. These parameters complete the spectral characteristics obtained on these same radicals during the first part of this work by flash photolysis. These thermodynamic data confirm the behavior observed in flash photolysis: the electronic transfer, which occurs during catechin photooxidation, involves selectively the cycle offering the lower redox potential, i.e., the catechol B-ring. Theoretical calculations of the stability of the various catechin radicals (Table 7) confirm these trends: the 4′-phenoxyl radical, corresponding to the more easily oxidizable phenolate, is the most stable radical, and the radicals can be ordered with regard to their values ($E_{PhO^\circ} - E_{PhO^-}$) characterizing the electron affinity in the following sequence: 4′-OH, 3′-OH, 7-OH, 5-OH, which corroborates the redox properties determined by ultramicroelectrode voltammetry.

D. Chemical Reactivity of Phenoxyl Radical: From ns to ms Range. To investigate the overall reactivity of phenoxyl radical, it is particularly interesting to combine results from flash photolysis and cyclic voltammetry experiments. Indeed, the first one, flash photolysis, allows the characterization of short-lived intermediates down to 200 ns and so the characterization of their initial chemical reactivity, while the second one, electrochemistry, permits the characterization of the reactivity at a

(39) Wayner, D. D. M.; Lusztyk, E.; Page, D.; Ingold, K. U.; Mulder, P.; Laarhoven, L. J. J.; Aldrich, H. S. *J. Am. Chem. Soc.* **1995**, *117*, 8737.
(40) Wayner, D. D. M.; Lusztyk, E.; Ingold, K. U.; Mulder, P. *J. Org. Chem.* **1996**, *61*, 6430.
(41) Arends, I. W. C. E.; Louw, R.; Mulder, P. *J. Phys. Chem.* **1993**, *97*, 7914.
(42) Wright, J. S.; Carpenter, D. J.; McKay, D. J.; Ingold, K. U. *J. Am. Chem. Soc.* **1997**, *119*, 4245.
(43) (a) Corse, J.; Ingraham, L. L. *J. Am. Chem. Soc.* **1951**, *73*, 5706. (b) Cohen, L. A.; Jones, W. M. *J. Am. Chem. Soc.* **1963**, *85*, 3397. (c) Pearce, P. J.; Simkins, J. J. *Can. J. Chem.* **1968**, *46*, 241.
(44) (a) Agrawal, P. K.; Schneider, H. J. *Tetrahedron Lett.* **1983**, *24*, 177. (b) Jarosszewski, J. W.; Matzen, L.; Frolund, B.; Krogsgaard, P. *J. Med. Chem.* **1996**, *39*, 515. (c) Berger, S. *Tetrahedron* **1981**, *37*, 1607. (d) Haran, R.; Nepveu-Juras, F.; Laurent, J. P. *Org. Magn. Reson.* **1979**, *12*, 153. (e) Maciel, G. E.; James, R. V. *J. Am. Chem. Soc.* **1964**, *86*, 3893.

Scheme 6

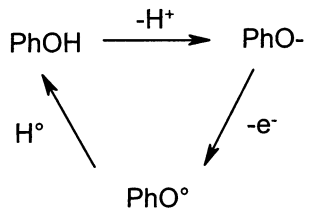

longer time range by the determination of the mechanism of the reaction following the first electronic transfer.

Our flash photolysis study allows, thus, for the first time, the determination of the intrinsic reactivity of each ring of catechin: H-abstraction involves mainly the A-ring, while the photooxidation is selective on the B-ring. These results clearly show that the electronic transfer, which occurs during photooxidation and the H-atom transfer are radically different and characteristic of the specific reactivity of each cycle of catechin. This chemical behavior implies a kinetic and not a thermodynamic control of the H-abstraction reaction. This is readily deduced from the examination of the physical−chemical parameters pK_a, $E°$, and BDE. Indeed, if we consider the thermodynamic cycle depicted in Scheme 6, we can notice that the three parameters pK_a, $E°$ (controlling thermodynamically the photooxidation), and BDE (expected to be correlated to the H-abstraction process) are correlated. However, we have demonstrated in the second part of this work that the standard potential of each phenolic function follows the same trends as that of the pK_a: the more acidic ring (B-ring) is related to the more oxidizable one (Tables 6 and 7). So this ring would also present the lowest O−H dissociation energy (BDE). This hypothesis is corroborated by theoretical calculation of O−H bond strength reported in Table 5. Indeed, as expected, the two phenolic functions 3′ and 4′ on the B-ring present the lowest BDE. So, the selectivity of H-abstraction on the A-ring is due to a kinetic control of the reaction.

Furthermore, the cyclic voltammetry at low scan rate allows us to examine in detail the intrinsic chemical behavior of each phenolic function by the study of the mechanism of the reaction following the electronic transfer, when the previous one is fast enough not to be the kinetically determinant step of the consecutive reaction. This favorable case appeared for two of our compounds, models of A- or B-ring, respectively. The major problem encountered during this kind of study comes from the dependence of the studied mechanism with the concentration. For example, at very low concentration, the oxidative coupling of coniferyl alcohol leads mainly to the formation of carbon−oxygen bonds found in lignin, while at higher concentration, it is the formation of carbon−carbon bonds which occurs.[21d] So several mechanisms, more particularly the DIM 2 ones—found for the compound offering only the 4′ phenolic function free—are quite difficult to characterize.

The study of the reactivity of the catechol B-ring shows that the methylation of one of the two *o*-hydroxyl functions excludes the dismutation leading to the formation of an *o*-quinone usually observed during catechol oxidation. Yet, the dimerization radical−phenolate found on our trimethylated analogue of catechin can be encountered, for the same reasons, during the oxidation of the B-ring monomethylated metabolites present in plasma.

To our best knowledge, the reactivity of the A-ring during oxidation has never been studied until now. However, the chemical behavior of this resorcinol-like ring is of great interest since it controls the synthesis of condensed tannins present notably in many fruits.[45] So, this work shows that the first step of the radical coupling is a DIM 1 reaction, i.e., a coupling between two phenoxyl radicals but the complete understanding of the mechanism leading to the biosynthesis of condensed tannins requires the analysis of the products formed upon oxidation experiments realized at physiological concentration to characterize the behavior as close as possible to the biochemical process.

Conclusions

The physical chemistry and the free radical chemistry of flavan-3-ols have been extensively investigated by laser flash photolysis and cyclic voltammetry studies. This study allowed thus (i) the identification of the structure of the two flavan-3-ol radical families, (ii) the determination of all the thermodynamic constants of each phenolic function of flavan-3-ols, namely, redox potential and microscopic dissociation constants, and (iii) the characterization of the intrinsic reactivity of each ring at different time scale. The overall results, useful and indispensable in discussing biological and biochemical phenomenon, permits us to propose a new insight into the antioxidative properties of flavan-3-ols.[11h]

Acknowledgment. This work was supported by the European Community (European Contract QLK1-CT-199-00505 POLY-BIND) and the Conseil Régional Nord, Pas-de-Calais.

Supporting Information Available: Optimized geometries calculated at the B3LYP/6-31G* level for catechin, its 4′-phenoxyl radical and 4′-phenolate and charge and spin distribution on optimized geometries of catechin, radical phenoxyls, phenolates, and radical anions of catechin (PDF). This material is available free of charge via the Internet at http://pubs.acs.org.

JA0262434

(45) Haslam, E. *Plant Polyphenols: Vegetable Tannins Revisited (Chemistry and Pharmacology of Natural Products)*; Cambridge University Press: Cambridge, U.K., 1990.